INTERMEDIATE AND STABLE REDOX STATES OF CYTOCHROME c STUDIED BY LOW TEMPERATURE RESONANCE RAMAN SPECTROSCOPY

BO CARTLING
Department of Biophysics, Arrhenius Laboratory, Stockholm University, S-106 91 Stockholm, Sweden

ABSTRACT Stabilized intermediate redox states of cytochrome c are generated by radiolytic reduction of initially oxidized enzyme in glass matrices at liquid nitrogen temperature. In the intermediate states the heme group is reduced by hydrated electrons, whereas the protein conformation is restrained close to its oxidized form by the low-temperature glass matrix. The intermediate and stable redox states of cytochrome c at neutral and alkaline pH are studied by low-temperature resonance Raman spectroscopy using excitations in resonance with the B (Soret) and Q_1 (β) optical transitions. The assignments of the cytochrome c resonance Raman bands are discussed. The observed spectral characteristics of the intermediate states as well as of the alkaline transition in the oxidized state are interpreted in terms of oxidation-state marker modes, spin-state marker modes, heme iron—axial ligand stretching modes, totally symmetric in-plane porphyrin modes, nontotally symmetric in-plane modes, and out-of-plane modes.

INTRODUCTION

Intermediate redox states of electron transfer enzymes, generated upon change of the oxidation state as states in which the protein has not relaxed to the equilibrium conformation corresponding to the new oxidation state, might play an important role in biological energy conversion processes (1, 2). To establish the existence and characteristics, such as the molecular nature and lifetime, of such intermediate states, resonance Raman (RR) spectroscopy appears to be a particularly useful technique. It has been applied extensively to biological systems (3–6), in particular to heme proteins, which exhibit richly structured spectra, that have been proven sensitive to oxidation state, spin state, heme iron—axial ligand interactions, and other protein influences on the heme group. We have recently performed time-resolved RR studies of the kinetics of the redox transition of cytochrome c (cyt c). Both the reduction by hydrated electrons generated by pulse radiolysis (7) and the chemical reduction by sodium dithionite in a continuous mixed flow experiment (8) were studied. It appears desirable to obtain more detailed spectral characterizations of the intermediate states by improving the resolution and signal-to-noise ratio, which can be obtained by the time-resolved studies. For this purpose the present work describes the RR analysis of intermediate states of cyt c stabilized at low temperature. A glycerol and aqueous buffer mixture serves as a glass matrix for cyt c at liquid-nitrogen temperature. The enzyme, initially in its oxidized form, is reduced by hydrated electrons generated by irradiating the solution with high-energy electrons. The heme group is reduced, whereas the protein conformation is restrained close to its oxidized form by the glass matrix

at the low temperature. RR spectroscopy provides much more detailed information than a previous analysis by optical absorption spectroscopy (9, 10) of cyt c prepared in an analogous manner.

EXPERIMENTAL

Chemicals

The cyt c was from horse heart (type VI; Sigma Chemical Co., St. Louis, MO) and was used without further purification. All samples were of concentration 1 mM unless otherwise stated. The glass matrices were 1:1 (vol/vol) mixtures of glycerol and an aqueous buffer. The glycerol was of spectrophotometric grade (Aldrich Chemical Company, Inc., Milwaukee, WI). The buffers were 50-mM sodium phosphate at pH = 7.0 and 50-mM glycine/NaOH at pH = 10.8. Buffer components (Merck, Darmstadt, Federal Republic of Germany) as well as $K_3Fe(CN)_6$ (Merck) and $Na_2S_2O_4$ (Fisons Scientific Apparatus, Loughborough, Leics., England) used for chemical oxidation and reduction of cyt c, respectively, were all of analytical grade, and water was distilled and deionized.

RR Spectroscopy

Continuous-wave lasers were used for excitation of RR spectra, a Spectra Physics Kr+-ion laser at 413.1 nm (model 170; Spectra-Physics Inc., Mountain View, CA) and a Coherent Radiation Ar+-ion laser at 514.5 nm (model CR4; Coherent Inc., Palo Alto, CA). The exciting light was filtered by a double prism, passed through an iris and focused by a plano-convex cylindrical lens, focal length 100 mm, onto the sample via a mirror in a 180° backscattering geometry. Scattered light was collected by an NIKKOR-S Auto 1:1.4 lens (Nikon Inc., Instrument Div., Garden City, NY), focal length 50 mm, giving a magnification of 6 at the entrance slit of the spectrometer in combination with a plano-convex spherical lens, focal length 300 mm. As a polarization scrambler a quartz wedge (Spex Industries, Inc., Metuchen, NJ) was used. The spectrometer consisted of a Jobin-Yvon HG2 Ramanor double 1-m monochromator (Instruments S. A., Inc., Metuchen, NJ) with concave holographic

gratings, a RCA C31034-A02 GaAs-type photomultiplier tube (RCA Electro-Optics and Devices, RCA Solid State Div., Lancaster, PA) cooled to $-25°C$, a Brookdeal-Ortec 9511 quantum photometer (EG&G Ortec, Oak Ridge, TN) and a Nicolet 1074 signal averager (Nicolet Instrument Corp., Madison, WI) and a PDP 11 minicomputer (Digital Equipment Corp., Maynard, MA) linked to a DEC 10 computer (Digital Equipment Corp.) for accumulating and processing spectra.

Spectra were recorded using a laser power of ~100 mW at the sample (Dewar flask, see the Low Temperature Techniques section). To obtain a spectral resolution of ~3 cm^{-1}, entrance and exit slits of the double monochromator were set at 200 μm for 413.1-nm excitation and at 400 μm for 514.5-nm excitation. In both cases a scan rate of 100 cm^{-1}/min and a channel width of the multichannel analyzer of 1 cm^{-1} were used, but for 413.1-nm excitation four scans were accumulated, whereas two scans were accumulated for 514.5-nm excitation. Although the noise level of the spectra is extremely low, they were subjected to a 7-point binomial smooth so as to provide accurate band frequencies without substantial loss of resolution. Frequencies were calibrated by means of an indene sample just prior to any scan and are believed accurate within ±1 cm^{-1}.

Radiolysis

The irradiation of the samples with high-energy electrons to produce the intermediate states was performed with a 2 MeV Van de Graaff accelerator. A total dose of ~6 Mrad was obtained by irradiating for 4 min 27 s with 12.5 pulses of electrons/s, each pulse of width 2 μs and providing a dose of 1.8 krad. The excess hydrated electrons not utilized for reduction of cyt c and trapped in the low temperature glass matrices, giving rise to a deep blue color of the irradiated samples, were photobleached upon exposure to the laser light used for the RR analysis.

Low Temperature Techniques

Sample solutions were contained in a blown bulb (outer diameter ~4 mm, inner diameter ~3 mm) at the end of fused silica tubes. The sample tubes were sealed with plastic caps since sealing by a H_2/O_2 burner caused reduction of the cyt c, presumably from the intense ultraviolet radiation emitted from the melting quartz. The sample tubes were immersed in liquid nitrogen in small quartz Dewar flasks, one at the target position of the electron accelerator for irradiation and one in the sample compartment of the RR spectrometer for analysis. Ice-free liquid nitrogen is crucial since any ice particles easily adsorb onto the sample tubes and make the RR analysis impossible. As another measure to avoid ice formation on the sample tubes, and also to avoid any relaxation of the intermediate states to the stable reduced states, all transfers between different Dewar flasks (irradiation, storage, and RR analysis) were performed within liquid nitrogen by means of a small tube containing liquid nitrogen. To avoid boiling the liquid nitrogen throughout the scan of a RR spectrum, which would contribute significant noise, the temperature of the liquid nitrogen was lowered by temporarily lowering the pressure in the Dewar flask prior to a scan, allowing some of the liquid nitrogen to boil off, and then letting the pressure return to atmospheric.

RESULTS AND DISCUSSION

RR Spectra of Cytochrome c in Low Temperature Glass Matrices

The RR spectra of cyt c in glass matrices of 1:1 (vol/vol) mixtures of glycerol and an aqueous buffer at liquid-nitrogen temperature are shown in Figs. 1–4. The aqueous buffers used (specified in the Experimental section) were at pH = 7.0 for spectra in Figs. 1 and 3 and at pH = 10.8 for spectra in Figs. 2 and 4. Spectra in Figs. 1 and 2 were excited by a continuous-wave Kr$^+$-ion laser at 413.1 nm

close to resonance with the B (Soret) optical absorption band, whereas spectra in Figs. 3 and 4 were excited close to resonance with the Q_1 (β) band by a continuous-wave Ar$^+$-ion laser at 514.5 nm. Spectra a and c in Figs. 1–4 were obtained from the stable chemically oxidized and reduced forms of cyt c, respectively, whereas spectra b are from the radiolytically generated intermediate redox forms. Spectra a in Figs. 1 and 2 are expanded by ~2 relative to spectra b and c of the same figures, and spectra a in Figs. 3 and 4 are expanded by ~10 relative to spectra b and c of these figures. As discussed in the following section on Control Experiments the concentration of cyt c was increased to 10 mM in the samples used for spectra a in Figs. 3 and 4 from 1 mM in other samples to reduce the relative contributions from glycerol. The intensity of cyt c RR bands is not changed by this because of a compensation between increased scattering and increased absorption. No background subtractions have been made, the total background is indicated by the vertical bar at the right end of the spectra.

Control Experiments

Low Temperature and Solvent Effects. The eight spectra of the stable redox forms were also obtained at room temperature by a spinning-cell technique using the same spectral resolution of the double monochromator and other recording conditions also identical. A comparison shows that the lowering of the temperature narrows RR bandwidths and reduces the background and noise levels to provide spectra of higher resolution and better signal-to-noise ratio. There is, however, no obvious new structure revealed in the higher quality spectra that would rather reflect an influence of the solvent or the low temperature on the protein structure. No frequency shifts beyond the experimental accuracy are detected. We thus conclude that the glass matrices provide proper environments for the protein at low temperature. The glycerol/aqueous buffer type of matrix has been used for a long time (11) for low-temperature optical absorption spectroscopy.

Background Contributions. Glycerol itself has a rich Raman spectrum, with the most intense bands at 857, 1,062, and 1,466 cm^{-1}, when obtained exactly like the low-temperature spectra of cyt c with the exception of the exclusion of cyt c. However, this spectrum is not resonance enhanced by 413.1 or 514.5-nm excitation, and moreover it is suppressed by the optical absorption of cyt c. In the B-band excited spectra of the stable reduced forms a weak band is seen only at 1,062 cm^{-1} of the glycerol frequencies, from which we conclude that the glycerol does not contribute to these spectra. From this fact and since the intensity of the strongest band of the B-band excited spectra is only reduced by $\sim\frac{1}{2}$ from the stable reduced to the oxidized forms, and the optical absorption by cyt c at the glycerol RR bands is not drastically changed between the oxidation
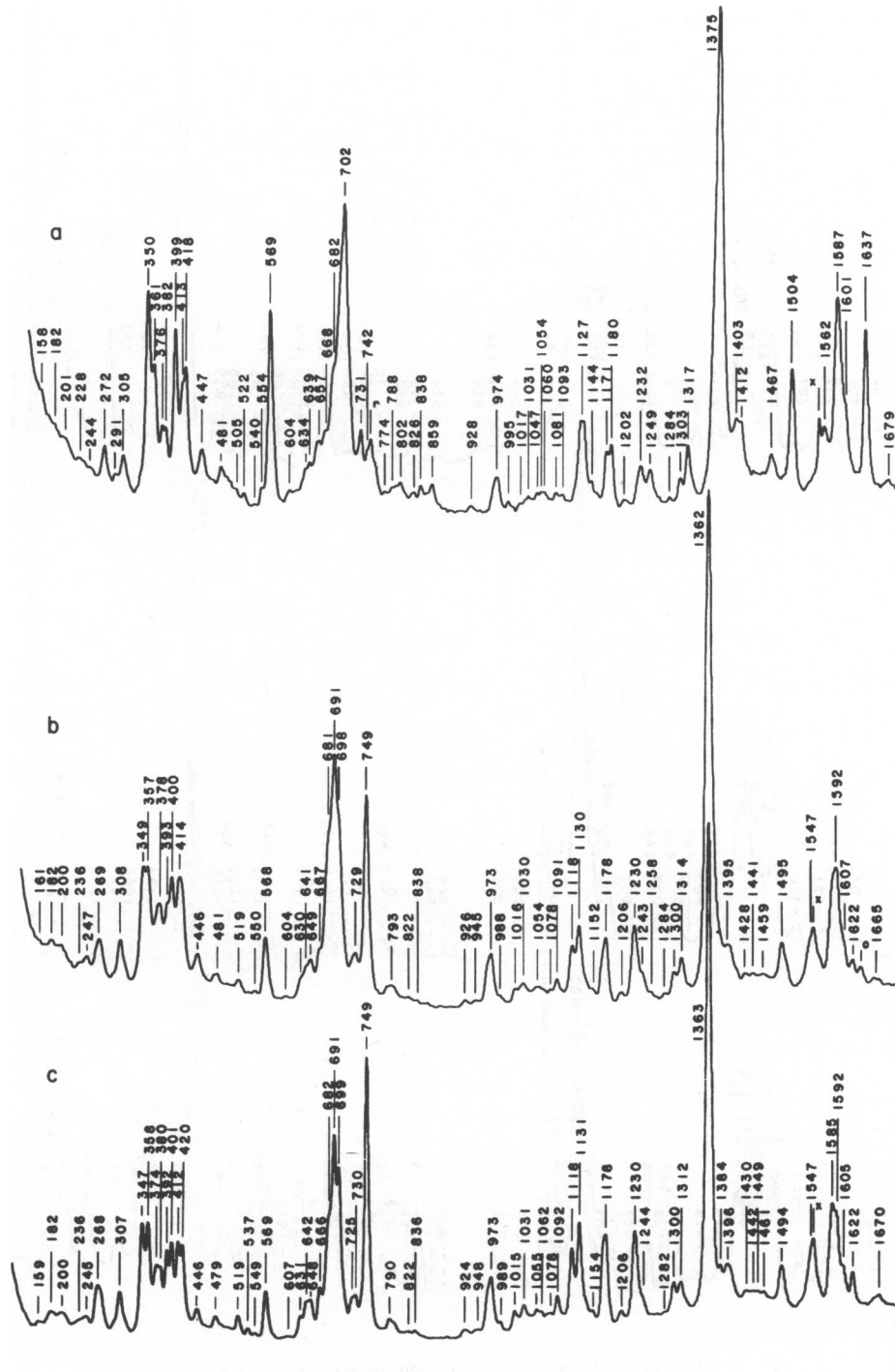
FIGURE 1 Resonance Raman spectra of cytochrome *c* in a glycerol/aqueous buffer (pH – 7.0) glass matrix at 77 K excited by a continuous-wave Kr⁺ ion laser at 413.1 nm; (*a*) chemically oxidized state, spectrum is expanded ~2; (*b*) radiolytically generated intermediate redox state; (*c*) chemically reduced state. Contributions from other than cyt *c* of the proper redox states are discussed in the Results and Discussion sections Control Experiments: *Background Contributions* and *Purity of Redox States*, and are denoted by *r*, reduced form; *o*, oxidized form; and *x*, liquid oxygen. All the details regarding the sample preparations and recording conditions are to be found in the Experimental section.
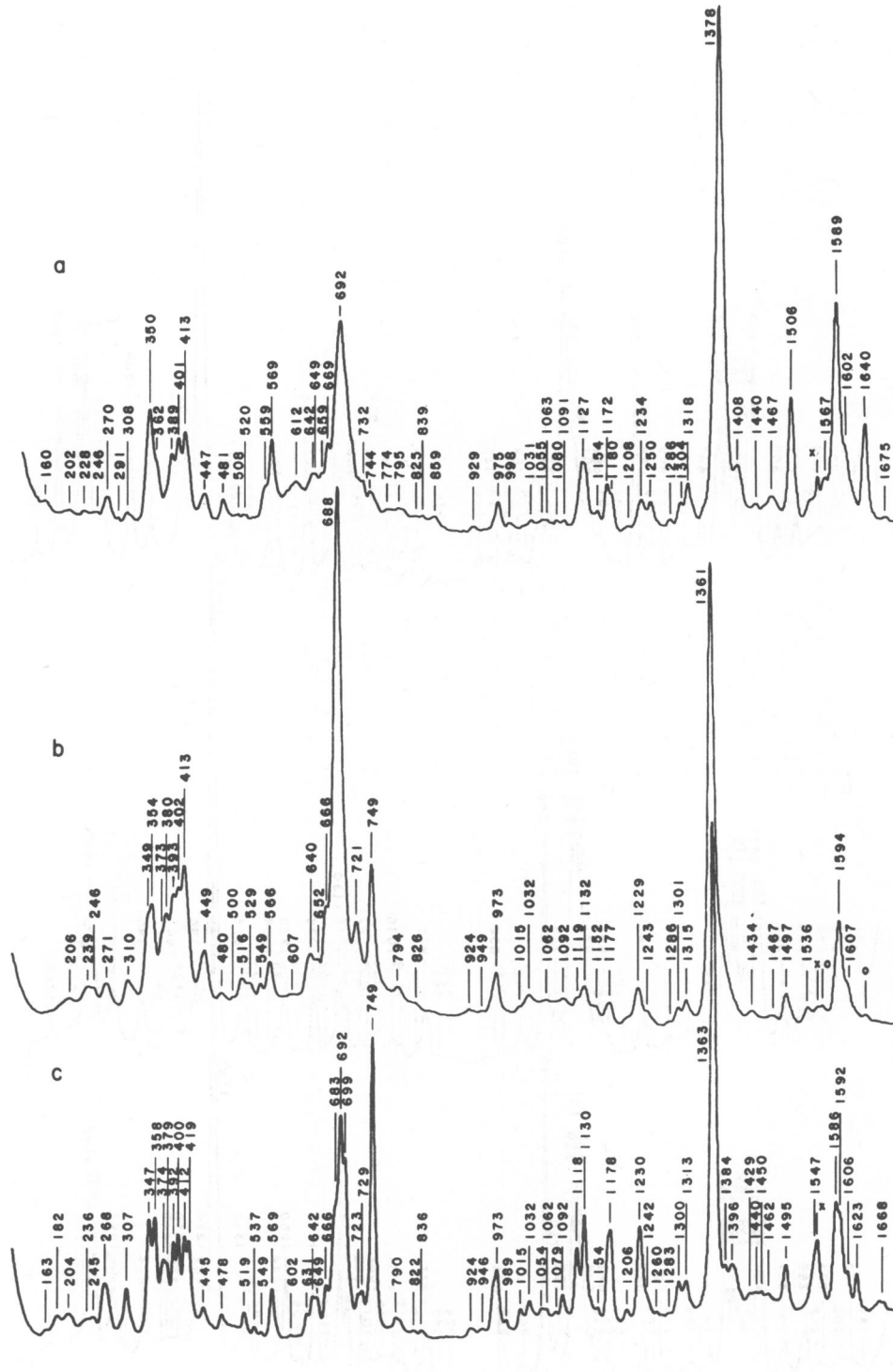
FIGURE 2   As in Fig. 1, but aqueous buffer at pH = 10.8.

states, we do not expect the glycerol bands to appear in the spectra of the oxidized forms. It was also confirmed by a comparison with B-band excited room-temperature spectra of solutions without glycerol that the bands in the low-temperature spectra at ~859, 1,062, and 1,467 cm^{-1} for the oxidized forms and at 1,062 cm^{-1} for the stable

reduced forms are real cyt c bands of expected intensity. Of the Q_1-band excited spectra the only ones in which glycerol bands appear are spectra a in Figs. 3 and 4, which were obtained from the oxidized forms that scatter 514.5-nm exciting light comparatively weakly. To reduce the relative contributions from glycerol to these spectra the cyt c
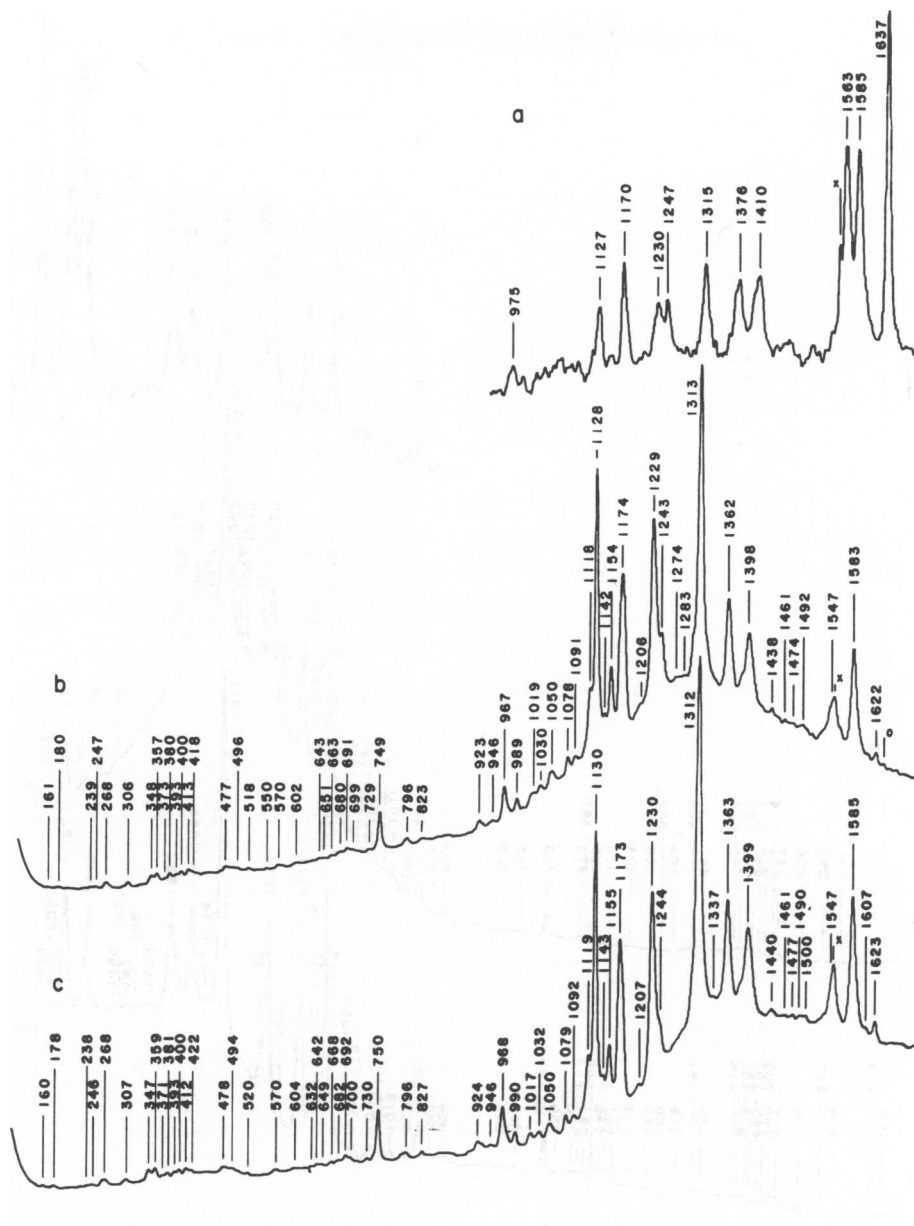
FIGURE 3 As in Fig. 1, but RR spectra excited by a continuous-wave Ar⁺ ion laser at 514.5 nm and spectrum *a* is expanded ~10. See the Results and Discussion section RR Spectra of Cytochrome *c* in Low Temperature Glass Matrices for particular remarks on the recording of spectrum *a*.

concentration was increased to 10 mM in these samples. Regarding irradiated glycerol see the section on *Irradiation Effects*.

Other chemical components of the solutions were present in concentrations too low to contribute Raman bands. It was verified that ferricyanide, which has a strong absorption at 420 nm (ϵ = 1,050 M^{-1} cm^{-1}), does not contribute resonance-enhanced bands during 413.1-nm excitation.

As the scattered-light intensity from cyt *c* is optimized, a part of the exciting-light focal cylinder falls within the liquid nitrogen. The stretching mode of the N_2 molecule in

the liquid phase is detectable as a Raman line at 2,327 cm^{-1}, which is outside the frequency range of interest here. The liquid nitrogen used, however, contained a small proportion, ~0.3% (molar), of liquid oxygen that produces a weak Raman line at 1,553 cm^{-1}. In the spectra of the oxidized forms, this band does not interfere with other bands and is easily distinguished. However, in those spectra where one cyt *c* band is located at 1,547 cm^{-1}, this band is slightly skewed by a minor contribution from the oxygen band as marked in these spectra. The frequency of this cyt *c* band was determined by subtraction of the oxygen band measured separately. By immersing the sample within
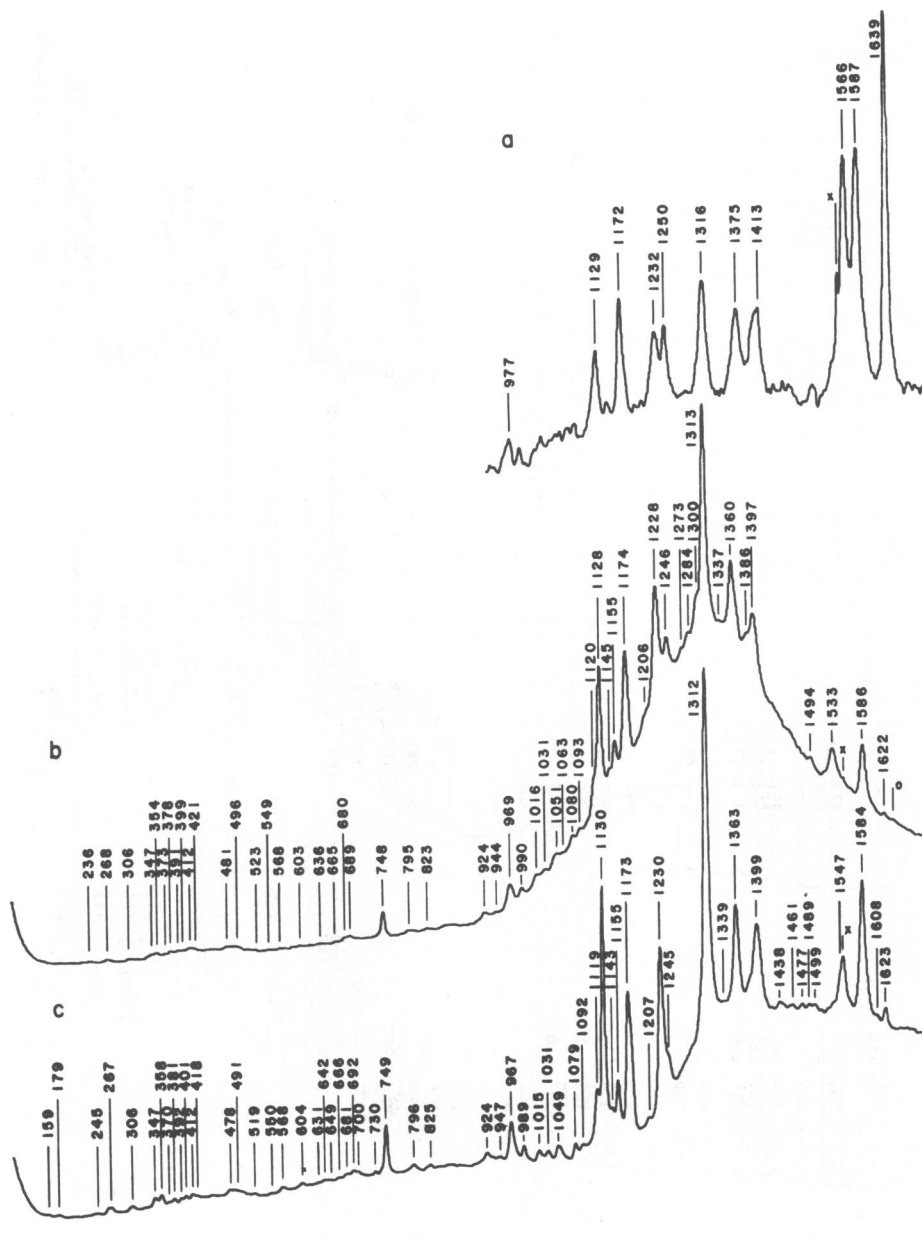
FIGURE 4 As in Fig. 3, but aqueous buffer at pH = 10.8.

liquid nitrogen rather than cooling it at a cold finger, a lower temperature is maintained when the exciting light is absorbed under the resonance conditions employed. This reduces the possibility of relaxation of the intermediate states to the stable reduced states during exposure to the laser light and also improves the quality of the spectra.

With the backscattering geometry used, the spectra are susceptible to include contributions from plasma lines from the ion gas lasers. The strongest lines would be at 914 cm^{-1} from the Kr$^+$ laser and at 520 cm^{-1} from the Ar$^+$ laser, as determined in the context of the above-mentioned investigations of Raman scattering from liquid nitrogen. There is a band at ~520 cm^{-1} in B-band excited spectra and the weak band at this frequency in Q$_1$-band excited spectra is

not stronger than expected from cyt c itself as estimated by a comparison with neighboring bands in B-band excited spectra that also appear in Q$_1$-band excited spectra. We thus conclude that the double prism filtering and iris used in the exciting-light path and the cyt c absorption together make neither of the plasma lines contribute significantly to any of our spectra.

The silica of the sample tubes is another possible contributor of Raman bands in the backscattering experiments. Its major bands are located at 426, 487, 598, and 790 cm^{-1}. They are all, except 487 cm^{-1}, broad features, but even an influence on the baseline is not detected in the spectra shown, where the low frequency region of the weak Q$_1$-band excited spectra of the oxidized forms is excluded.

Purity of Redox States. Up to 10% of the cyt *c* as purchased was in the stable reduced form. In producing the oxidized forms by chemical oxidation with potassium ferricyanide, we observed a photoreduction of cyt *c* by 413.1-nm laser light in the presence of any excess ferricyanide. The fraction of cyt *c* reduced in this way exhibited the same B-band excited RR spectra as did the radiolytically generated intermediate redox states. Removal of excess ferricyanide by gel filtration on a Sephadex G-25 fine column (Pharmacia Fine Chemicals Div., Pharmacia Inc., Piscataway, NJ) leaves a small proportion, typically ~3%, in the reduced form. Instead of such purification, by adding the appropriate amount of ferricyanide, the total proportion of stable reduced and intermediate forms, initially present and photolytically generated, respectively, could be limited to ~1%.

Weak contributions to the spectra of the intermediate forms at the frequencies 1,637 and 1,640 cm^{-1} for neutral and alkaline pH, respectively, indicate the presence of a small amount of oxidized cyt *c* that has not been reduced by the hydrated electrons. From the intensity of these bands, it can be estimated that ~90% of the originally oxidized cyt *c* has been reduced. The irradiation dose was not increased further as a measure to minimize any unwanted irradiation effects on the protein, see the following section on *Irradiation Effects*. The sample handling, keeping it immersed in liquid nitrogen throughout all steps of the experiments, ensures that there is no relaxation of the intermediate states to the stable reduced states. In particular, there is no such relaxation detected during the exposure to the laser light. The spectra of the stable reduced forms exhibit no indications of any presence of oxidized forms. Any bands deriving from other than the proper redox forms are clearly marked in the spectra, and any influence from such forms on the intensity of other bands is not sufficient to account for the spectral characteristics discussed in the sections on RR Spectral Characteristics.

Irradiation Effects. To verify that neither direct interactions between the high-energy electrons and cyt *c* nor effects of hydrated electrons on parts of the protein other than the heme group influence the results, the following control experiments were performed. By allowing the intermediate forms to relax by thawing the samples at room temperature and then analyzing them at liquid nitrogen temperature, RR spectra indistinguishable from those of chemically reduced cyt *c* were obtained. Irradiation of already chemically reduced samples by the same dose used for production of the intermediate states caused no observable changes in the RR spectra. The relatively low concentration of cyt *c* ensures that the abundant water molecules provide the major cross sections for the interaction with the ionizing radiation.

It has been observed that the radicals formed from glycerol in an aqueous solution during pulse radiolysis at room temperature do not reduce cyt *c* (12, 13). Moreover, at liquid-nitrogen temperature, chemical reduction by any molecular species is inhibited. The RR spectrum of the glycerol/aqueous buffer solvents used do not acquire any new bands when the solvents are irradiated by the same dose used for the generation of the intermediate states.

Assignments of Cytochrome *c* RR Bands

The RR spectra excited at 413.1 and 514.5 nm, close to resonance with the B (Soret) and Q_1 (β) optical transitions, respectively, provide complementary information to each other on the normal modes of cyt *c* (14, 15). Since these absorption bands originate from porphyrin π–π^* transitions (16, 17) polarized in the porphyrin plane, Raman scattering from in-plane porphyrin modes is most strongly enhanced. In D_{4h} symmetry they belong to the representations A_{1g}, A_{2g}, B_{1g}, B_{2g}, and E_u, all of which except for E_u are Raman active. Scattering from totally symmetric A_{1g} modes is selectively enhanced during excitation at 413.1 nm. The A-term scattering mechanism (18–20), in which only the excited state of the B optical transition is involved, is then operative and the scattered light is polarized. During 514.5 nm excitation, the scattering mechanism is of B-term type (18–20) based on a vibronic coupling between the two excited states of the B and Q optical transitions. The selection rules for the vibronic coupling imply that the active modes are of symmetries A_{1g}, A_{2g}, B_{1g}, and B_{2g}. A_{1g} modes are, however, not scattering efficiently by this mechanism (21). A_{2g} modes produce anomalously polarized scattering, whereas B_{1g} and B_{2g} modes generate depolarized scattering.

Since the scattered light from cyt *c* in a low-temperature glass matrix becomes essentially depolarized, it is not possible to determine depolarization ratios, but on the basis of reported polarization measurements (14, 22), the major RR bands of cyt *c* can be correlated with the observed fundamentals of the model compound Ni-octaethylporphyrin (NiOEP). The latter bands have all been assigned (23) and the composition of the normal modes has been determined by a normal coordinate analysis (24). The resulting assignments of the cyt *c* bands are summarized in Table I. The major contributions to the modes in the high-frequency region, 1,000–1,700 cm^{-1}, are from stretching vibrations of, in order of decreasing bond strength, C_b—C_b, C_a—C_m, C_a—N, C_b—substituent and C_a—C_b bonds and from C_m—H in-plane bending. C_a and C_b denote the inner and outer carbon atoms of the pyrrole rings, respectively, C_m the methine bridge carbons, N the pyrrole nitrogens, and H the methine bridge hydrogens. The low-frequency region, below 1000 cm^{-1}, is dominated by porphyrin deformation modes and by bending of the C_b—substituent bonds.

The infrared E_u modes might become Raman active as the porphyrin substituents and the rest of the protein remove the fourfold in-plane symmetry of the porphyrin. Several low-frequency E_u modes have been assigned to RR

TABLE I
ASSIGNMENTS OF CYTOCHROME c RR BANDS

Observed frequency cyt c (Fe^{2+}) (excitation)	Polarization*	Symmetry	Mode number‡	NiOEP§ frequency		NiOEP§ normal coordinate analysis potential energy distribution‖
				observed	calculated	
268 (B)	p (22)	A_{1g}	ν_9	226	230	23% $\delta(C_b{-}E_t)$, 16% $\nu(C_a{-}C_m)$
347 (B)	p (22)	A_{1g}	ν_8	344	326	57% $\delta(C_b{-}E_t)$, 11% $\nu(C_a{-}C_m)$
691 (B)	p (22)	A_{1g}	ν_7	674	655	20% $\delta(C_b{-}C_a{-}N)$, 19% $\nu(C_a{-}C_b)$
750 (Q$_1$)	dp (14)	B_{1g}	ν_{16}	751	741	14% $\delta(C_a{-}N{-}C_a)$, 14% $\nu(C_b{-}E_t)$
796 (Q$_1$)	p (14)	A_{1g}	ν_6	806	809	36% $\delta(C_a{-}C_m{-}C_a)$, 27% $\nu(C_a{-}N)$
1,118 (B)	p (22)	A_{1g}	ν_5	1,025	1,048	38% $\nu(C_b{-}E_t)$, 23% $\nu(C_a{-}C_b)$
1,130 (Q$_1$)	ap (14)	A_{2g}	ν_{22}	1,121	1,118	37% $\nu'(C_a{-}N)$, 26% $\nu'(C_b{-}E_t)$
1,173 (Q$_1$)	dp (14)	B_{1g}	ν_{14}	—	1,095	31% $\nu(C_a{-}C_b)$, 30% $\nu(C_b{-}E_t)$
1,230 (Q$_1$)	dp (14)	B_{1g}	ν_{13}	1,220	1,262	67% $\delta(C_m{-}H)$, 22% $\nu(C_a{-}C_b)$
1,312 (Q$_1$)	ap (14)	A_{2g}	ν_{21}	1,308	1,281	53% $\delta'(C_m{-}H)$, 18% $\nu'(C_a{-}C_b)$
1,363 (B)	p (22)	A_{1g}	ν_4	1,383	1,386	53% $\nu(C_a{-}N)$, 21% $\delta(C_a{-}C_m)$
1,399 (Q$_1$)	ap (14)	A_{2g}	ν_{20}	1,397	1,409	29% $\nu'(C_a{-}N)$, 24% $\nu'(C_b{-}E_t)$
1,494 (B)	p (22)	A_{1g}	ν_3	1,519	1,517	41% $\nu(C_a{-}C_m)$, 35% $\nu(C_a{-}C_b)$
1,547 (Q$_1$)	dp (14)	B_{1g}	ν_{11}	1,576	1,587	57% $\nu(C_b{-}C_b)$, 16% $\nu(C_b{-}E_t)$
1,585 (Q$_1$)	ap (14)	A_{2g}	ν_{19}	1,603	1,600	67% $\nu'(C_a{-}C_m)$, 18% $\nu'(C_a{-}C_b)$
1,592 (B)	p (22)	A_{1g}	ν_2	1,602	1,591	60% $\nu(C_b{-}C_b)$, 19% $\nu(C_b{-}E_t)$
1,623 (Q$_1$)	dp (14)	B_{1g}	ν_{10}	1,655	1,656	49% $\nu(C_a{-}C_m)$, 17% $\nu(C_a{-}C_b)$

*Numbers in parentheses refer to references.
‡Mode numbering as in references 23 and 24.
§NiOEP = Ni-octaethylporphyrin; from references 23 and 24.
‖Notations: ν = stretch, δ = in-plane bend, ν' and δ' are antisymmetric with respect to the C_2-axis of a pyrrole ring. Atoms denoted as in Results and Discussion section Assignment of Cytochrome c RR Bands, E_t = ethyl.

bands of bis-imidazole ferrous protoporphyrin IX ([ImH]$_2$Fe^{II}PP) at 558, 588, 717, 925, and 995 cm^{-1}.[1] In the low-frequency region there are also contributions from out-of-plane modes (see footnote 1). For a porphyrin of D_{4h} symmetry these belong to the A_{1u}, A_{2u}, B_{1u}, B_{2u}, and E_g representations, of which only the E_g modes are Raman active. Resonance enhancement, however, requires a vibronic coupling between an in-plane E_u and an out-of-plane A_{2u} optical transition. The A_{2u} charge transfer optical absorption band near 457.9 nm has permitted detection of the methine hydrogen out-of-plane deformation at 841 cm^{-1} in (ImH)$_2$Fe^{II}PP (see footnote 1). As the mirror plane symmetry of the porphyrin is lost because of substituents and the rest of the protein, A_{2u} modes also become RR active. Out-of-plane deformations of the methine carbon and of the C_b—substituent link have been assigned to bands at 298 and 384 cm^{-1}, respectively, in (ImH)$_2$ Fe^{II}PP, the latter mode also coupled to pyrrole tilting at 254 cm^{-1} (see footnote 1). Folding of the pyrrole rings, which are expected to be sensitive to heme-protein interactions, appear in all the out-of-plane symmetries. The enhancement of scattering from A_{1u}, B_{1u}, and B_{2u} modes not only requires symmetry lowering by a lost mirror plane, but also vibronic coupling between in-plane

optical transitions and is therefore not expected to be strong. The bands at 426, 488, and 507 cm^{-1} in (ImH)$_2$Fe^{II}PP have been assigned to pyrrole folding modes (see footnote 1).

We make no specific correlations between the observed cyt c RR bands and the in-plane E_u modes and various out-of-plane modes discussed above. The account of these assignments merely is intended to indicate the approximate frequency range for various contributions. Since all the substituents are saturated and therefore not involved in the porphyrin π conjugation, resonance enhancement by the π–π^* optical transitions is expected to be low for substituent modes. The interesting question of heme iron—axial ligand stretching modes will be considered in the Interpretations of the Observed RR Spectral Characteristics section.

RR Spectral Characteristics of the Alkaline Transition of Oxidized Cytochrome c

It is well established that oxidized cyt c undergoes an isomerization with a pK of ~9.3 (25). In the alkaline form the Met-80 that serves as sixth ligand to the heme iron at neutral pH is displaced. The heme iron remains in a low spin state and the favored candidate for the new, strong field ligand required for this is Lys-79 or Lys-72. The recent high-resolution x-ray crystallographic structure determination of cyt c and its associated water molecules has allowed a more detailed description of the alkaline

[1]Choi, S., and T. G. Spiro. 1983. Out-of-plane deformation modes in the resonance Raman spectra of metalloporphyrins and heme proteins. *J. Am. Chem. Soc.* In press.

transition (26, 27). A buried water molecule in the heme crevice weakens the Fe—S (Met-80) bond. A second water molecule, in the alkaline form of OH^-, is electrostatically attracted by the ferric iron to break the weakened Fe—S bond. The replacement of OH^- with Lys-79 (or Lys-72) is a slower process involving major structural rearrangements of the protein. These are suggested to be facilitated by breakage of the hydrogen bond between the buried water molecule and O (Thr-78) as OH^- replaces Met-80. An indicator of the displacement of Met-80 is the disappearance of the charge transfer optical transition, porphyrin a_{2u} (π) to Fe $a_{1g}(d_z2)$ at 695 nm (25, 28). From measured titration curves of this absorption band, we have established that the glycerol added in our experiments does not shift the pK of the alkaline transition appreciably. Electron paramagnetic resonance studies (29) indicate the existence of two alkaline forms of oxidized cyt c, although the proposed second form with lysine residues as both fifth and sixth ligand to the heme iron appears difficult to obtain. In the reduced state of cyt c the Met-80 remains as sixth ligand even at alkaline pH. At a higher pK, ~12, there is a second isomerization that affects the reduced state as well (25), but our pH = 10.8 is chosen to be well below that transition.

The transition of oxidized cyt c from pH = 7.0 to pH = 10.8 is accompanied by several changes of the RR spectrum as evident from comparisons of spectra a in Figs. 1 and 2 from B-band excitation and of spectra a in Figs. 3 and 4 from Q_1-band excitation. Shifts of some high-frequency bands have previously been observed in Q_1-band excited spectra (30). These and other indications of the alkaline transition are seen in the B-band excited spectra. All the bands that have been distinguished to serve as oxidation state markers (15), i.e., those at 1,375, 1,504, 1,562, and 1,637 cm^{-1} in the oxidized state of the neutral form of cyt c, undergo shifts upwards to 1,378, 1,506, 1,567, and 1,640 cm^{-1}, respectively. In the low-frequency region there are in particular two intervals that change drastically. One is ~680–700 cm^{-1}, where there are three components distinguished in the stable reduced state; a major band at 691 cm^{-1}, a less intense but resolved band at 699 cm^{-1} and a shoulder at 682 cm^{-1}. In the oxidized state the most intense of these bands is at 702 cm^{-1} in the neutral form and at 692 cm^{-1} in the alkaline form. The other low-frequency interval is ~350–420 cm^{-1}, where four doublets appear in the stable reduced state. All but one of these components are present in the spectrum of the neutral form of oxidized cyt c though with different relative intensities from those in the stable reduced state. In the alkaline form, however, the spectrum exhibits a completely different structure; in particular the bands at 376 and 382 cm^{-1} have disappeared. In the stable reduced state there is no major conformational transition in the pH interval studied. Hydrogen-bond interactions are susceptible to changes in pH, but we do not observe any significant influences on the spectra of the stable reduced forms.

RR Spectral Characteristics of the Intermediate Redox States of Cytochrome c

Intermediate redox states were produced by irradiating oxidized cyt c in glycerol/aqueous buffer glass matrices at liquid-nitrogen temperature with high-energy electrons from an electron accelerator, as described in detail in the Experimental section. The heme group is then reduced by hydrated electrons produced by the ionizing irradiation, whereas the main part of the protein is restrained close to its oxidized conformation by the low-temperature glass matrix.

The RR spectra from the intermediate redox forms of cyt c indeed reflect that the heme group is reduced since these spectra (Figs. 1–4 b) show greater similarity to those from the stable reduced forms (Figs. 1–4 c) than to those from the stable oxidized forms (Figs. 1–4 a). The RR spectral characteristics of the intermediate states are therefore described below as frequency shifts and intensity changes of RR bands with reference to the spectra from the stable reduced forms.

At Alkaline pH. A comparison of the B-band excited spectra as seen in Fig. 2 b, c provides numerous indications of the existence of an intermediate state. The most striking difference is the enormous enhancement in the intermediate state of the band located at 692 cm^{-1} in the stable reduced state, which also is shifted to 688 cm^{-1}. It is also not possible to detect any shoulders at ~683 and 699 cm^{-1} where there are bands in the stable reduced state, but they might of course be unresolved below the giant 688-cm^{-1} band. The intensity of the strong band at 749 cm^{-1} in the stable reduced state is considerably lowered in the intermediate state. Within the nearby pair of bands at 723 and 729 cm^{-1} in the stable reduced state is an increase of the intensity of the low-frequency component in the intermediate state and any high-frequency component is not resolved. Also in the low-frequency region the four doublets between 347 and 419 cm^{-1} in the stable reduced state are drastically different in the intermediate state. The pair at 347 and 358 cm^{-1} in the stable reduced state is of lower intensity in the intermediate state, particularly the 347-cm^{-1} band. The 374-cm^{-1} band in the stable reduced state is also lowered in the intermediate state, whereas the 412-cm^{-1} band is raised so that any band corresponding to the 419-cm^{-1} band in the stable reduced state cannot be resolved. In the interval between 445 and 569 cm^{-1}, a combination of frequency shifts and intensity changes produces several differences. In the very low-frequency region the most obvious difference is the disappearance in the intermediate state of the bands at 163 and 182 cm^{-1} in the stable reduced state. There is also an increase in the intermediate state of the band located at 236 cm^{-1} in the stable reduced state.

In the high-frequency region the most prominent indication of an intermediate state is the change of the band

located at 1,547 cm^{-1} in the stable reduced state. This change is, however, even more distinct in the Q_1-band excited spectra dicussed below. The dominant band in B-band excited spectra of the stable redox forms, the oxidation state marker positioned at 1,363 cm^{-1} in the stable reduced state, is slightly shifted to 1,361 cm^{-1} in the intermediate state. The bands at 1,586 and 1,623 cm^{-1} in the stable reduced state are not present in the intermediate state. The more pronounced shoulder at 1,243 cm^{-1} is another feature of the intermediate state more clearly observed in the Q_1-band excited spectrum.

In the Q_1-band excited spectra the most prominent difference is the frequency shift of the band at 1,547 cm^{-1} in the stable reduced state to 1,533 cm^{-1} in the intermediate state. The second strongest indication of an intermediate state is the increased intensity of the band at 1,246 cm^{-1}. A decreased intensity is observed for the band that is located at 1,623 cm^{-1} in the stable reduced state. All these three features of the intermediate state are observed in the B-band excited spectrum as discussed above, although the first two are more clearly distinguished in the Q_1-band excited spectrum. There is also an increase of the intensity of the shoulders at 1,300 and 1,386 cm^{-1} in the intermediate state. The more intense and more peaked fluorescence background in the Q_1-band excited spectrum of the intermediate state relative to that of the stable reduced state appears to be a real feature of the intermediate state because it returns to that of the stable reduced state upon relaxation of the intermediate state to the stable reduced state by thawing of the samples.

The observed characteristics of an intermediate state at alkaline pH include those observed in our kinetic studies of the redox transition of cyt c by time-resolved RR spectroscopy (7, 8). This fact indicates that the molecular nature of the intermediate state stabilized at low temperature in the present investigation is similar to that of the transient states observed during pulse radiolytic (7) or chemical (8) reduction at room temperature.

At Neutral pH. A corresponding analysis of the neutral form of cyt c reveals fewer and weaker indications of the existence of an intermediate redox state. In the neutral form of cyt c there is no drastic conformational change upon a redox transition as in the alkaline form. Indeed, only minor structural rearrangements between oxidized and reduced equilibrium conformations have been detected by high-resolution x-ray crystallography (26, 27). Functionally cyt c is also not expected to undergo any large energy transferring conformational transitions during its redox cycle because it mainly serves as an intermediary electron shuttle in the respiratory chain of mitochondria (25).

The RR spectral evidences for an intermediate redox state of cyt c at neutral pH are the following. In the B-band excited spectra there is a reversal of relative intensities of

the bands that are located at 691 and 749 cm^{-1} in the stable reduced state. Within the pairs of bands at 374–380, 392–401, 412–420, 725–730, and 1,585–1,592 cm^{-1} in the stable reduced state, the relative intensity of the components at 374, 392, 420, 725, and 1,585cm^{-1} is lowered in the intermediate state. There is also a lowering of the intensity in the intermediate state of the band at 1,622 cm^{-1} in the stable reduced state. In the Q_1-band excited spectrum there is a distinct increase of the shoulder at 1,243 cm^{-1} in the intermediate state.

Some of these effects are similar to but less pronounced than those observed for the intermediate state of the alkaline form. This might be due to the origins of these effects being of a similar nature although present to a different degree in the two intermediate states. However, there might be a possibility that during the radiolysis of the neutral solution of cyt c a small fraction of the Fe—S (Met-80) bonds have been broken prior to the heme reduction. The evidences available opposing such an interpretation of the indications of an intermediate state at neutral pH are the following. The decrease of the intensity of the band located at 392 cm^{-1} in the stable reduced state relative to that of the 401 cm^{-1} band is unique to the intermediate state at neutral pH, i.e., not observed in the alkaline case. Whereas the low frequency component of the doublet at 725 and 730 cm^{-1} in the stable reduced state is of lower relative intensity in the intermediate state at neutral pH; the low-frequency component is enhanced to the extent that any high-frequency component is not resolved at alkaline pH.

Interpretations of the Observed RR Spectral Characteristics

Oxidation-State Marker Modes. The RR bands that have been distinguished to serve as oxidation state markers (15), i.e., those at 1,363, 1,494, 1,547, and 1,623 cm^{-1} in the stable reduced state, are all assigned as porphyrin stretching modes, see Table I, ν_4 and ν_3 of A_{1g} symmetry and ν_{11} and ν_{10} of B_{1g} symmetry, respectively. In the oxidized state of the neutral form of cyt c, these bands are located at 1,375, 1,504, 1,563, and 1,637 cm^{-1}, respectively. The frequency shifts between oxidation states are interpreted in terms of π back donation from the Fe $e_g(d_\pi)$ orbitals to the porphyrin $e_g(\pi^*)$ orbitals (15). Such π back donation is diminished in the oxidized state due to the lowering of the Fe $e_g(d_\pi)$ energy level, which causes an increase of the force constants of these porphyrin stretching modes. The pattern of bond changes upon occupation of either of the orbitals that constitutes a basis of the porphyrin $e_g(\pi^*)$ state is of B_{1g} symmetry. This fact in combination with a dynamic Jahn-Teller effect, operative upon partial occupancy of this degenerate state, make B_{1g} modes the most susceptible to frequency changes (6). The further shift of frequencies upwards to 1,378, 1,506, 1,566,

and 1,639 cm^{-1}, respectively, upon the alkaline transition in the oxidized state indicates a further reduction of π back donation in the alkaline vs. the neutral form of oxidized cyt c. As sixth ligand to the heme iron, Met-80 in the neutral form acts as a weak π-donor, whereas Lys-79 (or Lys-72) in the alkaline form is π-nonbonding, which is consistent with the trend observed. In the intermediate state at alkaline pH, where the heme iron is reduced but Lys-79 remains as sixth ligand, frequencies shift downward because the raised Fe $e_g(d_\pi)$ level allows more π back donation. The ν_4, ν_3, ν_{11}, and ν_{10} bands are located at 1,361, 1,497, 1,533, and 1,622 cm^{-1}, respectively. With ν_3 as an exception, frequencies thus are lower in the intermediate state at alkaline pH than in the stable reduced state. The dependence on sixth ligand thus is reversed from what is observed when the heme iron is oxidized. The major difference between the two oxidation states is the location of the Fe $e_g(d_\pi)$ energy level. In the oxidized state, when the level is low, it appears suitably located for charge transfer from the π-level of S(Met-80). The high position of the Fe $e_g(d_\pi)$ level, when the iron is reduced, seems to favor a strong σ-bonding with N(Lys-79) that diffuses the Fe $e_g(d_\pi)$ orbitals and thus allows a larger overlap with the porphyrin $e_g(\pi^*)$ orbitals.

In particular the large frequency shift of the B_{1g} mode ν_{11} between the intermediate state at alkaline pH and the stable reduced state is distinguished as an indicator of the intermediate state. This mode is also shifted to 1,533 cm^{-1} in the stable reduced state of dicarboxymethylated cyt c at alkaline pH (31, 32). In this modified form of cyt c, where Met-65 and Met-80 are carboxymethylated, Met-80 is displaced as sixth ligand to the heme iron in both oxidation states at alkaline pH, and Lys-79 is believed to be the replacing ligand (33). This observation thus supports our interpretation of the intermediate state as one in which the protein conformation is close to that of the oxidized state.

In addition to the electronic effects of ligand substitution, the protein conformational change might also influence the porphyrin normal modes through the thioether linkages of two cysteine residues to pyrrole C_b atoms. According to the normal coordinate analysis of the model compound NiOEP (24), the main components of the ν_{11} mode is 57% C_b—C_b stretching and 16% C_b—substituent stretching. That the electronic effects discussed above dominate is suggested by the dependence on various ligands of the ν_{11} frequency of model compounds. In particular (ImH)$_2$Fe^{II}PP, in which the sixth ligand is N(ImH) with similar bonding properties to N(Lys-79), has its ν_{11} frequency at 1,534 cm^{-1} (34), close to where we observe it in the intermediate state at alkaline pH.

Spin State Marker Modes. The bands that have been observed to shift their frequencies appreciably between low and high spin states of heme proteins (15) are those denoted ν_{19}, ν_{10}, ν_3, and ν_2 in Table I. Both the oxidized

and the stable reduced state of cyt c at neutral pH are low spin, $S = 1/2$ and $S = 0$, respectively (35). The frequency shifts we observe for these spin-state marker modes upon the alkaline transition of oxidized cyt c or between the intermediate states and the stable reduced states are maximally 2 cm^{-1}, which is less than significant for a spin change. The low spin character of the oxidized state at alkaline pH (25) is thus confirmed and of the intermediate states is established. It has been noted (36, 37) that ν_{19}, ν_{10}, and ν_3 respond to the porphyrin core size, specifically to the porphyrin center-N(pyrrole) distance, through their contribution from methine bridge bending. Our results thus indicate an essentially preserved porphyrin-core size upon the alkaline transition of the oxidized form and between the intermediate states and the stable reduced states. Apart from these modes all skeletal modes above 1,450 cm^{-1} have been shown to correlate similarly to the porphyrin-core size (38). One of the additional modes, ν_{11} and ν_2, of those in Table I that implies, ν_{11}, does show distinct frequency shifts, in particular between the intermediate state at alkaline pH and the stable reduced state but also upon the alkaline transition of the oxidized form. These shifts, however, are fully accounted for by the electronic effects of the change of the sixth ligand to the heme iron as discussed in the *Oxidation-State Marker Modes* section.

Heme Iron—Axial Ligand Stretching Modes. Additional, more direct evidences of the switch of the sixth ligand to the heme iron in the alkaline transition of oxidized cyt c and between the intermediate state at alkaline pH and the stable reduced state would be the observation of changes in the heme iron—axial ligand stretching modes. These have so far not been identified for cyt c, but it is possible that the present investigation can contribute to the identification. Because the two ligands to the heme iron are not equivalent, both of the two stretching modes are Raman active. Resonance enhancement, in particular during B-band excitation, can be expected because stretching of the Fe—ligand bonds modulates the π back donation to the porphyrin $e_g(\pi^*)$ orbitals involved in the optical transition. The replacement of Met-80 as sixth ligand with Lys-79 (or Lys-72) would cause an upwards shift of the Fe—ImH (His-18) stretching frequency because the two Fe—ligand stretching modes are strongly coupled. Approximate frequencies of these modes can be estimated from a simple model, a linear triatomic molecule where the two ligands are replaced by effective point masses. The force constant of the Fe—ImH bond has been estimated as ~ 1.6 mdyn/Å from studies on the model compound (ImH)$_2$Fe^{II}PP, in which the Fe-ImH stretching frequency at 200 cm^{-1} has been identified from its perdeuteration shift (Mitchell, M., S. Choi, and T. G. Spiro, manuscript in preparation). The Fe—S (Met-80) bond force constant can be approximated by the value shown to fit the Fe—S (Cys) stretching frequencies in various

Fe—S proteins, where the Fe—S distance is very similar to the 2.32 Å determined by x-ray crystallography (26, 27) of the stable reduced cyt c, i.e., ~1.2 mdyn/Å (39).[2] The effective mass in atomic units of S (Met-80) is estimated to be 61 by including the first coordination sphere of atoms around S, that of Fe is estimated to be 56, and that of ImH(His-18) to be 82 by including a methyl group in the link to the protein. The estimated effective masses of the ligands represent compromises between lowered values due to the coupling of the Fe—ligand stretching modes with internal ligand modes and raised values because of the steric restrictions imposed by the linkages to the rest of the protein. From the specified model and parameters, the Fe—ImH and Fe—S stretching frequencies are calculated to be 182 and 344 cm^{-1}, respectively. The 182-cm^{-1} value is also close to the observed value of 179 cm^{-1} of the model compound bis-pyridine ferrous mesoporphyrin (40). For the situation when Met-80 is replaced by a lysine residue, the force constant of the Fe—N (Lys) bond can be approximated to be the same as for Fe—N (ImH) because the bonding properties of these nitrogen atoms to the iron are similar. An effective mass of the lysine residue is estimated to be 30 by including the first coordination sphere of atoms around the N atom. The calculated frequencies for the Fe—ImH (His-18) and the Fe—N (Lys) stretching modes are 232 and 408 cm^{-1}, respectively. Our observations that a band present at 182 cm^{-1} in the stable reduced state is absent in the intermediate state at alkaline pH, and that there is an increase of intensity in the intermediate state of the band located at 236 cm^{-1} in the stable reduced state in combination with the approximate model calculations suggest a tentative assignment of the 182 cm^{-1} band in the stable reduced state to the Fe—ImH (His-18) stretching mode. The Fe—S (Met-80) stretching frequency is then expected near 344 cm^{-1}, which is within a region of other strong bands making identification difficult. Also, the character of this mode is close to the antisymmetric stretching mode of a triatomic molecule with two equal ligands to the Fe atom that is not Raman active and therefore this band might be weak. The spectra of the oxidized forms are fairly weak in the lowest frequency region, but there is a weak indication of a band at 182 cm^{-1} in the neutral form, which is not seen in the alkaline form. The surprising fact that the Fe—ImH stretching frequency is independent of the iron oxidation state has been observed on the model compound $(ImH)_2Fe^{II}PP$ (Mitchell, M., S. Choi, and T. G. Spiro, manuscript in preparation). It might be due to a delocali-

zation of the extra electron added in the reduced state into the porphyrin $e_g(\pi^*)$ orbitals by π back donation as discussed in the Oxidation-State Marker Modes section.

Totally Symmetric In-Plane Modes. The intensity of scattered light from totally symmetric A_{1g} modes is determined by nuclear Franck-Condon factors (18–20). These make the intensity increase proportionally to the square of the origin shift of the corresponding mode between the ground and excited states of the optical transition, close to which the exciting laser light is in resonance.

The band that shows the most drastic change of intensity between the intermediate states and the stable reduced states, in particular at alkaline pH, i.e., the band located at 692 cm^{-1} in the stable reduced state, is assigned to an A_{1g} mode, ν_7 (see Table I). The major components of this mode are 20% C_b—C_a—N bending and 19% C_a—C_b stretching giving it the character of a breathing mode of the inner porphyrin ring. The intensity variation observed thus indicates a larger distortion similar to this inner ring breathing movement upon optical excitation in the intermediate state than in the stable reduced state.

Also the neighboring bands, located at 682 and 699 cm^{-1} in the stable reduced state, are determined to have polarized scattering (22) and thus should be assigned to A_{1g} modes. The observation that cytochrome b_{562}, which has the same axial ligands as reduced cyt c, but lacks the peripheral C—S (Cys) covalent linkages of the porphyrin, does not have two of the three bands discussed has been used (41) to propose the disappearing bands as candidates for C—S (Cys) stretching vibrations, and the ν_7 mode is associated with the remaining band, which in that protein is located at 680 cm^{-1}. The C—S (Cys) linkages are certainly susceptible to be influenced by conformational transitions of the protein, which might account for the intensity changes of these bands that we observe upon the alkaline transition of oxidized cyt c and between the intermediate states and the stable reduced states.

Nontotally Symmetric In-Plane Modes. According to the selection rules discussed in the Assignment of Cytochrome c RR Bands section, exciting light in resonance with the B optical absorption band is scattered polarized from A_{1g} modes. Polarization measurements on B-band excited RR spectra of cyt c (22) have, however, revealed depolarized and anomalously polarized bands of considerable intensity. Thus depolarized bands at 749, 1,230, and 1,622 cm^{-1} in the stable reduced state can be assigned to the B_{1g} modes, ν_{16}, ν_{13}, and ν_{10}, respectively, and an anomalously polarized band at 1,585 cm^{-1} to the A_{2g} mode ν_{19}. In fact, bands appear in the B-band excited spectra at positions of all the bands in the Q_1-band excited spectra that are assigned to B_{1g} and A_{2g} modes, i.e., ν_{14} and ν_{11} of B_{1g} symmetry at 1,178 and 1,547 cm^{-1} in the stable reduced state, and ν_{22}, ν_{21}, and ν_{20} of A_{2g} symmetry at 1,131,

[2]Yachandra, V. K., J. Hare, I. Moura, J. J. G. Moura, A. V. Xavier, and T. G. Spiro. 1983. Resonance Raman spectra of rubredoxin, desulforedoxin and the synthetic analog Fe $(S_2$-o-xyl)$_2^-$; conformational effects. *J. Am. Chem. Soc.* In press; Yachandra, V. K., J. Hare, A. Gewirth, R. S. Czernuszewicz, T. Kimura, R. H. Holm, and T. G. Spiro. 1983. Resonance Raman spectra of spinach ferredoxin and adrenodoxin, and of analog complexes. *J. Am. Chem. Soc.* In press.

1,312, and 1,396 cm^{-1}, respectively, in addition to the above-mentioned bands. An assignment of these bands in the B-band excited spectra to nontotally symmetric modes as an alternative to accidental degeneracies between modes of different symmetries requires an explanation as regards the scattering mechanisms. Vibronic coupling of the components of the degenerate B state was added to the vibronic interaction between the B and Q states to account for the appearance of depolarized modes in B-band excited spectra of metalloporphyrins (42). The Jahn-Teller type of excited-state distortions resulting from such vibronic coupling provide the origin shifts of the normal modes required for the Franck-Condon factors and thus the scattering intensity to be nonzero. The intensity of a band should increase with the excited-state distortion, but the depolarization ratio does not change by such a distortion. The observation that all the bands in our B-band excited spectra, which are suggested to be assigned to B_{1g} modes, are lower in intensity in the intermediate state at alkaline pH than in the stable reduced state, most dramatically for ν_{10}, which is no longer seen, thus indicates a smaller excited-state distortion of B_{1g} symmetry in the intermediate state. This is consistent with the similarity of the excited-state distortion to the A_{1g} mode ν_7 indicated by the enormous increase of intensity in the intermediate state as discussed in the *Totally Symmetric In-Plane Modes* section. In the alkaline transition of the oxidized form the intensities of these bands are lowered, which is also consistent with the observed increase of the intensity of the A_{1g} mode ν_7. A_{2g} modes, however, are not Jahn-Teller active in D_{4h}. As a mechanism for scattering of these modes in addition to vibronic coupling between the B and Q states, vibronic coupling between the components of the B state is possible in the lower symmetry D_{2h}. It has been established by low-temperature optical absorption spectroscopy (11) and by magnetic circular dichroism measurements (43) that the Q_0 band is split by ~100 cm^{-1}, and this has been ascribed to the inequivalence of the x and y directions in the porphyrin plane. The observed split might be partly due to a permanent distortion in the ground state from influences by the porphyrin substituents and the rest of the protein, and partly from a Jahn-Teller distortion in the excited state. In the lower symmetry D_{2h} of a distorted ground state, the components of the B state, which is of E_u symmetry in D_{4h}, belong to the B_{2u} and B_{3u} representations. Their direct product is B_{1g}, which also is the representation according to which an A_{2g} mode in D_{4h} is transformed in D_{2h}, making vibronic coupling of the B-state components a possible contribution to the scattering from these modes. A limited ground-state distortion makes the analysis above for B_{1g} modes in D_{4h} still applicable, though as a pseudo–Jahn-Teller effect.

Out-Of-Plane Modes. Many of the out-of-plane modes, such as the folding of the pyrrole rings and the wagging of the C_b—substituent links, are expected to be

sensitive to heme-protein interactions and thus to be useful monitors of protein conformational transitions. The various intervals of the low-frequency region where different types of out-of-plane modes are expected were indicated in the Assignments of Cytochrome c RR Bands section. Several of the observed characteristics of the alkaline transition of oxidized cyt c and of the intermediate states indeed fall in these frequency intervals.

The changed frequencies and intensities between the intermediate state at alkaline pH and the stable reduced state of the bands located at 445, 478, 519, and 537 cm^{-1} in the stable reduced state is one example, coinciding with the interval of bands at 426, 488, and 507 cm^{-1} in $(ImH)_2Fe^{II}PP$, suggested to correspond to pyrrole folding (see footnote 1). The wagging mode of the C_b—substituent links assigned to the 384-cm^{-1} band in $(ImH)_2Fe^{II}PP$ (see footnote 1) is in the center of the region where four doublets occur in the stable reduced state of cyt c, and several dramatic changes take place both in the alkaline transition of oxidized cyt c and in the transition between the intermediate states and the stable reduced states.

CONCLUSION

(a) Evidence that intermediate redox states of cytochrome c can be stabilized at liquid-nitrogen temperature by radiolytic reduction of initially oxidized enzyme in glycerol/aqueous buffer glass matrices can be obtained by resonance Raman spectroscopy. The heme group is reduced by hydrated electrons, whereas the protein conformation is restrained close to its oxidized form. (b) Resonance Raman spectra of high resolution and high signal-to-noise ratio can be obtained from cyt c in its intermediate and stable redox states by low temperature spectroscopy. (c) The major resonance Raman bands can be correlated with the observed fundamentals of the model compound Ni-octaethylporphyrin, which have all been assigned and characterized by a normal coordinate analysis. (d) Numerous spectral characteristics of the intermediate states as well as of the alkaline transition of oxidized cyt c can be distinguished. (e) The spectral characteristics of the intermediate state at alkaline pH indicate that the molecular nature of this state, as prepared in this study, is similar to that of the transient states observed in kinetic studies of the redox transition of cyt c at room temperature by time-resolved resonance Raman spectroscopy. (f) The frequency shifts of the oxidation-state marker modes between the intermediate states and the stable reduced states and upon the alkaline transition of oxidized cyt c can be explained by the π- and σ-donor properties of the Met and Lys residues, which alternately serve as the sixth ligand to the heme iron, in combination with π back donation from the Fe $e_g(d_\pi)$ orbitals to the porphyrin $e_g(\pi^*)$ orbitals, and the dependence of the Fe $e_g(d_\pi)$ energy level on the oxidation state. (g) The absence of frequency shifts of the spin state marker modes indicates an

unchanged low spin state as well as a preserved porphyrin core size between the intermediate states and the stable reduced states and upon the alkaline transition of oxidized cyt c. (h) Heme iron—axial ligand stretching frequencies can be estimated from a simple model, a linear triatomic molecule where the two ligands are replaced by effective point masses. These estimates in combination with the observed dependence of the sixth ligand suggest a tentative assignment of the band located at 182 cm^{-1} in the stable reduced state as the Fe—ImH (His-18) stretching frequency. (i) The enormous increase of intensity of the inner porphyrin-ring breathing A_{1g} mode in the intermediate state at alkaline pH as compared with the stable reduced state indicates a larger distortion similar to this mode upon B-band excitation in the intermediate state. (j) Depolarized bands from B_{1g} modes and anomalously polarized bands from A_{2g} modes appear with considerable intensity in B-band excited spectra. Vibronic coupling of the components of the B state can account for the appearance of B_{1g} modes because the resulting Jahn-Teller type of excited-state distortions provide the origin shifts required for the Franck-Condon factors to be nonzero. The intensity variations of the B_{1g} modes observed between the intermediate states and the stable reduced states and upon the alkaline transition of oxidized cyt c are consistent with the reverse intensity variations of the inner porphyrin-ring breathing A_{1g} mode. Vibronic coupling of the components of the B state can also contribute to the scattering from A_{2g} modes in the symmetry D_{2h}. (k) Frequency shifts and intensity changes are observed in the transition between the intermediate and the stable reduced states as well as in the alkaline transition of oxidized cyt c in frequency regions where out-of-plane modes such as folding of the pyrrole rings and wagging of the C_b—substituent links, which are expected to be useful monitors of protein conformational transitions, have been identified in the model compound bis-imidazole ferrous protoporphyrin.

REFERENCES

1. Blumenfeld, L. A. 1978. The physical aspects of energy transduction in biological systems. *Q. Rev. Biophys.* 11:251–308.
2. Cartling, B., and A. Ehrenberg. 1978. A molecular mechanism of the energetic coupling of a sequence of electron transfer reactions to endergonic reactions. *Biophys. J.* 23:451–461.
3. Spiro, T. G., and T. M. Loehr. 1975. Resonance Raman spectra of heme proteins and other biological systems. *In* Advances in Infrared and Raman Spectroscopy. R. J. H. Clark and R. E. Hester, editors. Heyden & Son, Ltd., London. 1:98–142.
4. Van Wart, H. E., and H. A. Scheraga. 1978. Raman and resonance Raman spectroscopy. *Methods Enzymol.* 49:67–149.
5. Carey, P. R., and B. R. Salares. 1980. Raman and resonance Raman studies of biological systems. *In* Advances in Infrared and Raman Spectroscopy. R. J. H. Clark and R. E. Hester, editors. Heyden & Son, Ltd., London. 7:1–58.
6. Spiro, T. G. 1983. The resonance Raman spectroscopy of metalloporphyrins and heme proteins. *In* Iron Porphyrins, Part Two. Physical Bioinorganic Chemistry Series, no. 2. A. B. P. Lever and H. B. Gray, editors. Addison-Wesley Publishing Co., Inc., Reading, MA. 89–159.
7. Cartling, B., and R. Wilbrandt. 1981. Time-resolved resonance Raman spectroscopy of cytochrome c reduced by pulse radiolysis. *Biochim. Biophys. Acta.* 637:61–68.
8. Forster, M., R. E. Hester, B. Cartling, and R. Wilbrandt. 1982. Continuous flow-resonance Raman spectroscopy of an intermediate redox state of cytochrome c. *Biophys. J.* 38:111–116.
9. Blumenfeld, L. A., R. M. Davydov, N. S. Fel', S. N. Magonov, and R. O. Vilu. 1974. Studies on the conformational changes of metalloproteins induced by electrons in water-ethylene glycol solutions at low temperature. Cytochrome c. *FEBS (Fed. Eur. Biochem. Soc.) Lett.* 45:256–258.
10. Davydov, R. M., S. N. Magonov, A. M. Arutyunyan, and Y. A. Sharonov. 1979. Absorption and magnetic circular dichroism spectra of heme-containing proteins in non-equilibrium states. IV. Cytochrome c and its derivatives. *Mol. Biol. (Mosc.).* 12:1037–1042.
11. Estabrook, R. W. 1956. The low temperature spectra of hemoproteins. I. Apparatus and its application to a study of cytochrome c. *J. Biol. Chem.* 223:781–794.
12. Simic, M. G., and I. A. Taub. 1977. Mechanisms of inter- and intra-molecular electron transfer in cytochromes. *Faraday Discuss. Chem. Soc.* 63:270–278.
13. Van Leeuwen, J. W., J. Tromp, and H. Nauta. 1979. Reduction of ferricytochrome c, methemoglobin and metmyoglobin by hydroxyl and alcohol radicals. *Biochim. Biophys. Acta.* 577:394–399.
14. Spiro, T. G., and T. C. Strekas. 1972. Resonance Raman spectra of hemoglobin and cytochrome c: Inverse polarization and vibronic scattering. *Proc. Natl. Acad. Sci. U.S.A.* 69:2622–2626.
15. Spiro, T. G., and T. C. Strekas. 1974. Resonance Raman spectra of heme proteins. Effects of oxidation and spin state. *J. Am. Chem. Soc.* 96:338–345.
16. Gouterman, M. 1959. Study of the effects of substitution on the absorption spectra of porphin. *J. Chem. Phys.* 30:1139–1161.
17. Gouterman, M. 1961. Spectra of porphyrins. *J. Mol. Spectrosc.* 6:138–163.
18. Albrecht, A. C. 1961. On the theory of Raman intensities. *J. Chem. Phys.* 34:1476–1484.
19. Tang, J., and A. C. Albrecht. 1970. Developments in the theories of vibrational Raman intensities. *In* Raman Spectroscopy. Theory and Practice. H. A. Szymanski, editor. Plenum Press, New York. 2:33–68.
20. Albrecht, A. C., and M. C. Hutley. 1971. On the dependence of vibrational Raman intensity on the wavelength of incident light. *J. Chem. Phys.* 55:4438–4443.
21. Perrin, M. H., M. Gouterman, and C. L. Perrin. 1969. Vibronic coupling. VI. Vibronic borrowing in cyclic polyenes and porphyrin. *J. Chem. Phys.* 50:4137–4150.
22. Champion, P. M., and A. C. Albrecht. 1979. Investigations of Soret excited resonance Raman excitation profiles in cytochrome c. *J. Chem. Phys.* 71:1110–1121.
23. Kitagawa, T., M. Abe, and H. Ogoshi. 1978. Resonance Raman

spectra of octaethylporphyrinato-Ni(II) and meso-deuterated and ^{15}N substituted derivatives. I. Observation and assignments of nonfundamental Raman lines. *J. Chem. Phys.* 69:4516–4525.

24. Abe, M., T. Kitagawa, and Y. Kyogoku. 1978. Resonance Raman spectra of octaethylporphyrinato-Ni(II) and meso-deuterated and ^{15}N substituted derivatives. II. A normal coordinate analysis. *J. Chem. Phys.* 69:4526–4534.

25. Dickerson, R. E., and R. Timkovich. 1975. Cytochromes c. *In* The Enzymes. P. D. Boyer, editor. Academic Press, Inc., New York. 11:397–547.

26. Takano, T., and R. E. Dickerson. 1981. Conformation change of cytochrome c. I. Ferrocytochrome c structure refined at 1.5 Å resolution. *J. Mol. Biol.* 153:79–94.

27. Takano, T., and R. E. Dickerson. 1981. Conformation change of cytochrome c. II. Ferricytochrome c refinement at 1.8 Å and comparison with the ferrocytochrome structure. *J. Mol. Biol.* 153:95–115.

28. Eaton, W. A., and R. M. Hochstrasser. 1967. Electronic spectrum of single crystals of ferricytochrome c. *J. Chem. Phys.* 46:2533–2539.

29. Brautigan, D. L., B. A. Feinberg, B. M. Hoffman, E. Margoliash, J. Peisach, and W. E. Blumberg. 1977. Multiple low spin forms of the cytochrome c ferrihemochrome. EPR spectra of various eukaryotic and prokaryotic cytochromes c. *J. Biol. Chem.* 252:574–582.

30. Kitagawa, T., Y. Ozaki, J. Teraoka, Y. Kyogoku, and T. Yamanaka. 1977. The pH dependence of the resonance Raman spectra and structural alterations at heme moieties of various c-type cytochromes. *Biochim. Biophys. Acta.* 494:100–114.

31. Ikeda-Saito, M., T. Kitagawa, T. Iizuka, and Y. Kyogoku. 1975. Resonance Raman scattering from hemoproteins: pH-dependence of Raman spectra of ferrous dicarboxymethyl-methionyl-cytochrome c. *FEBS (Fed. Eur. Biochem. Soc.) Lett.* 50:233–235.

32. Kitagawa, T., Y. Kyogoku, T. Iizuka, M. Ikeda-Saito, and T. Yamanaka. 1975. Resonance Raman scattering from hemoproteins. Effects of ligands upon the Raman spectra of various c-type cytochromes. *J. Biochem. (Tokyo).* 78:719–728.

33. Schejter, A., and I. Aviram. 1970. The effects of alkylation of methionyl residues on the properties of horse cytochrome c. *J. Biol. Chem.* 245:1552–1557.

34. Spiro, T. G., and J. M. Burke. 1976. Protein control of porphyrin conformation. Comparison of resonance Raman spectra of heme proteins with mesoporphyrin IX analogues. *J. Am. Chem. Soc.* 98:5482–5489.

35. Tasaki, A., J. Otsuka, and M. Kotani. 1967. Magnetic susceptibility measurements on hemoproteins down to 4.2° K. *Biochim. Biophys. Acta.* 140:284–290.

36. Spaulding, L. D., C. C. Chang, N.-T. Yu, and R. H. Felton. 1975. Resonance Raman spectra of metallooctaethylporphyrins. A structural probe of metal displacement. *J. Am. Chem. Soc.* 97:2517–2525.

37. Spiro, T. G., J. D. Stong, and P. Stein. 1979. Porphyrin core expansion and doming in heme proteins. New evidence from resonance Raman spectra of six-coordinate high-spin iron (III) hemes. *J. Am. Chem. Soc.* 101:2648–2655.

38. Choi, S., T. G. Spiro, K. C. Langry, K. M. Smith, D. L. Budd, and G. N. La Mar. 1982. Structural correlations and vinyl influences in resonance Raman spectra of protoheme complexes and proteins. *J. Am. Chem. Soc.* 104:4345–4351.

39. Geetharani, K., and D. N. Sathyanarayana. 1974. Infrared spectral assignments for transition metal thioxanthates. *Spectrochim. Acta. Part A Mol. Spectrosc.* 30:2165–2171.

40. Wright, P. G., P. Stein, J. M. Burke, and T. G. Spiro. 1979. Resonance Raman spectra, excitation profiles and excited (iron → pyridine charge transfer) state geometry of bispyridine iron (II) heme. *J. Am. Chem. Soc.* 101:3531–3535.

41. Yu, N.-T., and R. B. Srivastava. 1980. Resonance Raman spectroscopy of heme proteins with intensified vidicon detectors: studies of low frequency modes and excitation profiles in cytochrome c and hemoglobin. *J. Raman Spectrosc.* 9:166–171.

42. Cheung, L. D., N.-T. Yu, and R. H. Felton. 1978. Resonance Raman spectra and excitation profiles of Soret-excited metalloporphyrins. *Chem. Phys. Lett.* 55:527–530.

43. Sutherland, J. C., and M. P. Klein. 1972. Magnetic circular dichroism of cytochrome c. *J. Chem. Phys.* 57:76–86.